Received: 3 October 2023 | Revised: 22 December 2023 | Accepted: 15 January 2024

DOI: 10.1002/bit.28663

ARTICLE

BIOTECHNOLOGY AND BIOENGINEERING WILEY

A robust multinutrient kinetic model for enhanced lutein and biomass yields in mixotrophic microalgae cultivation: A step towards successful large-scale productions

Jihed Bentahar[1,2] | Jean-Sébastien Deschênes[1,2]

[1]Département de mathématiques, d'informatique et de génie, Collectif de recherche appliquée aux bioprocédés et à la chimie de l'environnement (CRABE), Université du Québec à Rimouski, Rimouski, Québec, Canada

[2]Département des sciences des aliments, Institut sur la Nutrition et les Aliments Fonctionnels (INAF), Faculté des sciences de l'agriculture et de l'alimentation, Université Laval, 2425, rue de l'Agriculture, Québec City, Québec, Canada

Correspondence

Jihed Bentahar, Département de mathématiques, d'informatique et de génie, Collectif de recherche appliquée aux bioprocédés et à la chimie de l'environnement (CRABE), Université du Québec à Rimouski, 300, Allée des Ursulines, Rimouski, Québec, G5L 3A1, Canada.
Email: jihed.bentahar2@uqar.ca

Funding information

Natural Sciences and Engineering Research Council of Canada; Institut sur la Nutrition et les Aliments Fonctionnels

Abstract

Mixotrophic cultivation holds great promise to significantly enhance the productivities of biomass and valuable metabolites from microalgae. In this study, a new kinetic model is developed, explicitly describing the effect of the most influential environmental factors on both biomass growth and the production of the high-value product lutein. This extensive study of multinutrient kinetics for *Tetradesmus obliquus* in a mixotrophic regime covers various nutritional conditions. Crucial nutrients governing the model include nitrate, phosphate, and glucose. Using seven state variables and 13 unknown parameters, the model's accuracy was ensured through a well-designed two-factor, four-level experimental setup, providing ample data for reliable calibration and validation. Results accurately predict dynamic concentration profiles for all validation experiments, revealing broad applicability. Optimizing nitrogen availability led to significant increases in biomass (up to fourfold) and lutein production (up to 12-fold), with observed maximum biomass concentration of 6.80 g L^{-1} and lutein reaching 25.58 mg L^{-1}. Noticeably, the model exhibits a maximum specific growth rate of 4.03 day^{-1}, surpassing reported values for photoautotrophic and heterotrophic conditions, suggesting synergistic effects. Valuable guidance is provided for applying the method to various microalgal species and results are large-scale production-ready. Future work will exploit these results to develop real-time photobioreactor operation strategies.

KEYWORDS

biomass production, lutein production, microalgae, mixotrophic conditions, multinutrient kinetic model

1 | INTRODUCTION

Unlocking the potential of microalgae as a revolutionary source of lutein ($C_{40}H_{52}O_2$), a highly coveted carotenoid compound, has recently garnered significant attention due to their often-remarkable lutein content, which even surpasses current commercial sources (e.g., marigold flowers) and offers unique advantages including year-round availability, reduced land and water requirements, and simplified extraction and purification processes (Chen, Chen, et al., 2019; Guedes et al., 2011). Rising interest in alternative sources of lutein stems from

its increasingly numerous industrial applications as a natural colorant (E161b) in various fields including food, animal tissues, drugs, and cosmetics (del Rio-Chanona et al., 2017). Furthermore, lutein has well-documented antioxidant and anti-inflammatory properties, which makes it a valuable bioproduct with high market demand. Notably, the lutein market in the United States was valued at USD 135 million in 2015 and is projected to grow 6% annually up to 2024, whereas the European Union's market is forecasted to nearly double from EUR 255 million in 2020 to EUR 409 million by 2027 (Chen, Chen, et al., 2019; Saha et al., 2020).

The primary challenge in harnessing microalgae for lutein production lies in the overall limited biomass and lutein yields. Despite successful commercial production of valuable carotenoids from other microalgal species, microalgal lutein production remains untapped (Saha et al., 2020). Overcoming yield limitations thus becomes imperative for achieving commercial viability. A recent review by Zheng et al. (2022) emphasizes the urgent need to identify high-yielding microalgal strains with a minimum lutein content of 5–10 g kg^{-1} while achieving much higher biomass productivities. Therefore, optimizing cultivation conditions to enhance the coproduction of biomass and lutein emerges as an indispensable step towards the economic feasibility and establishment of a commercially viable process.

This study pursues a promising solution that relies on a dual-pronged approach, combining mixotrophic cultivation and mathematical modeling to optimize cultivation conditions and enhance the coproduction of biomass and lutein. Mixotrophic cultivation, which utilizes both light and organic carbon as energy sources, has demonstrated its superiority over traditional photoautotrophic and heterotrophic methods, resulting in higher biomass productivities, growth rates, and cell densities (Yang et al., 2014). Additionally, mixotrophic conditions have been associated with the highest reported lutein production, as it positively correlates with growth (Zheng et al., 2022). On the other hand, mathematical modeling offers a robust engineering tool to help understand the intricate responses of microalgae to their growth environment, which can be used to increase the economic viability and sustainability of microalgal systems (Bekirogullari et al., 2020).

The freshwater microalga *Tetradesmus obliquus* is a perfect candidate for such a study as it is highly suited for mixotrophic conditions and has high lutein content (Oliveira et al., 2021). Channeling its full potential for high biomass and lutein production, however, will require a precise control of environmental factors such as nutrient availability. To this end, robust multifactorial kinetic models are usually necessary. In a previous study (Bentahar & Deschênes, 2022), significant progress was made in optimizing key nutrients, resulting in a notable increase in *T. obliquus* biomass, reaching up to 8 g L^{-1} in only 6 days. A first multinutrient model ($0.77 < R^2 < 0.99$) intended for biomass production was successfully developed (Bentahar & Deschênes, 2023). Improvements are however necessary for this model concerning nutrient kinetics (mainly for phosphate) and to obtain a mathematical description for the production of lutein. Both elements require new experimental data as compared to our previous studies. This, this study proposes an entirely new experimental plan (full factorial design) to develop an entirely new model. This represents a significant step forward, enhancing predictive capabilities for both biomass and lutein productivity across a wide range of conditions.

The study is organized as follows: first, the new experimental design for model calibration and validation is presented, using a two-factor, four-level design of experiments (4^2) with 16 trials and a 10-fold variation in nitrate and phosphate concentrations. Then, the mathematical structure of the model that was selected to describe the growth and lutein production kinetics of *T. obliquus* under mixotrophic conditions is illustrated, combining the Monod, Droop and Luedeking–Piret kinetic equations. The entire model includes seven state variables and 13 unknown parameters to be estimated. Next, the model's parameters were accurately estimated using a combination of Nelder–Mead and Levenberg–Marquardt methods, ensuring the model's reliability. Finally, the model's ability to predict and reproduce experimental data under various nutrient regimes was validated, confirming its utility as a powerful tool for optimizing and predicting mixotrophic microalgal cultivation of *T. obliquus* and potentially other microalgae species.

2 | MATERIAL AND METHODS

2.1 | Microalgae, media, and cultivation conditions

The microalga *T. obliquus* strain was obtained from the Canadian Phycological Culture Center at the University of Waterloo (Ontario, Canada). The medium used for cultivation was a modified version of Bold's Basal Medium (BBM), adjusted to an initial pH of 6.8 (Stein, 1973). The medium was supplemented with pure glucose at 10 g.L-1 as the sole organic carbon source in the mixotrophic mode. The experimental design involved the variation of concentrations for two critical components of BBM (i.e., nitrate and phosphate). The other BBM components (Table 1) were initially set at their optimum concentrations, as proposed by Bentahar and Deschênes (2022). All chemicals were obtained from Sigma-Aldrich and culture media were sterilized at 121°C for 20 min before use.

Batch mixotrophic cultivations were performed in 1 L Erlenmeyer flasks containing 600 mL of medium (working volume) in a Multitron II incubator shaker (INFORS HT). All manipulations were conducted under sterile conditions in a laminar flow biological hood. The cultivation conditions were maintained as follows: inoculation at 1×10^6 cells mL^{-1} (Day 0), temperature of 21°C, pH maintained at 7.20 using a 50 mM Tris-HCl buffer, continuous orbital agitation of 120 rpm, constant light intensity of 100 µmol m^{-2} s^{-1} and input CO_2 concentration of 1%. An overview of the systems is given in Figure 1.

2.2 | Experimental design

The experimental design employed in this study was built upon insights gained from our prior investigation (Bentahar & Deschênes, 2023). The

TABLE 1 Composition of modified BBM used for *Tetradesmus obliquus* mixotrophic growth, omitting nitrate and phosphate.

Nutrients	Concentrations	BBM's equivalent concentrations
Glucose (g L^{-1})	10.00	–
Sulfate (SO_4^-) (mg L^{-1})	309.89	10×
Chloride (Cl^-) (mg L^{-1})	122.40	5×
Magnesium (Mg^{2+}) (mg L^{-1})	37.06	5×
Calcium (Ca^{2+}) (mg L^{-1})	6.82	1×
Iron (Fe^{2+}) (mg L^{-1})	10.00	10×
Boron (BO_3^{3-}) (mg L^{-1})	10.38	1×
Manganese (Mn^{2+}) (mg L^{-1})	0.50	1×
Zinc (Zn^{2+}) (mg L^{-1})	0.05	1×
Molybdate (MoO_4^{2-}) (mg L^{-1})	0.26	1×
Copper (Cu^{2+}) (mg L^{-1})	0.02	1×
Cobalt (Co^{2+}) (mg L^{-1})	0.01	1×

Abbreviation: BBM, Bold's Basal Medium.

FIGURE 1 Batch cultivation experiments of *Tetradesmus obliquus* microalgae under mixotrophic conditions.

primary goal was to examine the influence of varying nitrate and phosphate concentrations on the biomass and lutein production of the microalga *T. obliquus* under mixotrophic conditions. In contrast to the earlier study, which utilized Taguchi's fractional factorial design incorporating nitrate, phosphate, and iron, the current approach deliberately narrows its focus to nitrate and phosphate due to the minimal impact of iron on the targeted parameters. This shift necessitated an entirely new set of experiments utilizing a 2^4 (two factors in four levels) full factorial design, carrying out 16 unique combinations and allowing for a more detailed exploration of the intricate relationships between nutrient intakes and the observed outcomes regarding growth and bioproducts. Nitrate and phosphate concentrations were systematically varied at four levels each (1×, 2×, 5×, and 10× BBM, as outlined in Tables 2 and 3), enabling a comprehensive

TABLE 2 Selected factors and their corresponding level settings.

Factor/nutrient	Level 1	Level 2	Level 3	Level 4
Nitrate (NO_3^-) (mg L^{-1})	182.4	364.8	912	1824
Phosphate (PO_4^{3-}) (mg L^{-1})	163.05	326.1	815.25	1630.5

Note: The four levels correspond to equivalent concentrations of 1×, 2×, 5×, and 10× Bold's Basal Medium, respectively, for each selected factor.

TABLE 3 Two-factor, four-level design of experiments (2^4) with 16 trials, $n = 2$.

Experimental runs	Level of factors (nutrients)	
	Nitrate	Phosphate
1	1	1
2	1	2
3	1	3
4[a]	1	4
5	2	1
6[a]	2	2
7	2	3
8	2	4
9[a]	3	1
10	3	2
11	3	3
12	3	4
13	4	1
14	4	2
15[a]	4	3
16	4	4

[a]The experiments utilized for model validation.

assessment of the effects of a 10-fold change in these factors on the model parameters. Although glucose was not varied as a factor in the experimental design, it was subsequently introduced as a state variable alongside nitrate and phosphate while developing the mathematical model for biomass and lutein production. Each case was conducted in duplicate ($n = 2$) to ensure the accuracy of the experimental data. Cultures were sampled twice a day during the growth phase and daily during the other phases for 12 days and analyzed using a variety of techniques, including ionic analysis, high-performance liquid chromatography (HPLC), and elemental analysis (C:H:N) to acquire the necessary data for model development and validation. Culture samples were centrifuged for 6 min at 3400 g to separate the cells from the supernatant, with the cell pellets used to determine biomass concentration, internal nitrogen and phosphorus cell quotas, and lutein content. In contrast, the supernatant was kept to measure glucose, nitrate, and phosphate concentrations.

2.3 | Analytical methods

To determine the biomass concentration, samples were washed twice with deionized water to remove excess salts, frozen at −80°C for at least 24 h and freeze-dried over 72 h at −46°C using a FreeZone 2.5 L Benchtop Freeze Dryer. The dried cell weight was then measured using a VWR analytical balance (±0.1 mg) to obtain the biomass concentration (g L^{-1}). The initial cell inoculum (Day 0) was manually counted using a hemacytometer (LW Scientific).

The internal nitrogen quota of the freeze-dried cells was quantitatively determined using a CHN elemental analyzer (COSTECH ECS 4010; Costech Analytical Technology) in conjunction with a zero blank autosampler and a reactor that converts the sample C and N to CO_2 and N_2, respectively. A standard calibration was established using acetanilide as a reference compound. The internal phosphorus quota of the algal cells was not measured directly but rather inferred based on the increment of algal biomass dry weight and the consumption of phosphate. Following mass balance principles in the cultivation system, the intracellular phosphorus content of algal cells was calculated as the ratio of phosphate uptake to the increment of algal biomass dry weight (Wu et al., 2013).

The algal pigments were extracted in 95% methanol, lysed by sonication (QSonica, Model Q125, 100 W) for 4 × 5 s on ice and centrifuged in an Eppendorf centrifuge (5430R, Eppendorf) at 6500 rpm for 5 min at 4°C. Extracts were filtered through a 0.2 µm polytetrafluoroethylene syringe filter and poured into an autosampler vial gently sparged with argon to limit oxidation. An Agilent 1200 series HPLC unit (Agilent Technologies) with a TSP UV 6000 LP diode-array absorbance detector (400–700 nm) and a Symmetry C8 column (150 × 4.6 mm, 3.5 µm particle size; Waters Corporation) was used for pigment separation as described in Zapata et al. (2000). Lutein was detected and quantified based on retention time and spectral properties of external pigment standards.

Measurement of the main anions (nitrate and phosphate) were determined by ion chromatography (Dionex Integrion RFIC, Thermo Scientific) equipped with an automated sampler (Dionex AS-AP Autosampler, Thermo Scientific). Separation and quantification were carried out using a Dionex IonPac AG18 (4 × 50 mm) guard column with a Dionex IonPac AS18 (4 × 250 mm) analytical column and a DRS Dionex ADRS 600 (4 mm) suppressor. The elution was obtained by the isocratic method at 30 mmol L^{-1} of KOH for 17 min. The flow rate was 1 mL min^{-1}, the sample injection volume was fixed at 12.5 µL and Chromeleon 7.2 SR5 software was used for data acquisition. The calibration was performed on standard solutions (all from Sigma-Aldrich) prepared in the concentration range of the samples to be analyzed.

The glucose concentrations in the supernatants were measured with an Agilent 1100 Infinity HPLC instrument. The HPLC was equipped with a Waters Sugar-Pak column (6.5 mm × 300 mm) and a refractive index detector was used. The column was maintained at a temperature of 90°C and the mobile phase consisted of 50 ppm EDTA (in Milli-Q water) with a flow rate of 0.5 mL min^{-1}. Samples were filtered through 0.45 µm nylon syringe filters before injection and the run time was 30 min. The calibration was performed using a range of standard solutions (from Sigma-Aldrich).

2.4 | Model construction and parameter estimation

A completely revised model was developed based on the recommendations of our previous research (Bentahar & Deschênes, 2022, 2023). The basic logic behind the revised model was similar to that used in the earlier model (Bentahar & Deschênes, 2023). Nitrate, glucose, and phosphate were selected as the key factors influencing both biomass and lutein synthesis since their productivity is closely correlated (Henríquez et al., 2016). Unlike the earlier model, the Droop model (Droop, 1968) was employed to characterize the storage of nitrogen and phosphorus in the form of internal quotas before their effective use for growth, whereas the classical Monod model (Monod, 1949) was applied to describe the impact of glucose. Description of mixotrophic growth rate and nutrient uptake rate were based on the multiplicative method that simultaneously allows all factors to affect the overall cell growth (Equations 1–3).

$$\mu(q_N, q_P, G) = \mu_{max}\left(1 - \frac{Q_{N\,min}}{q_N}\right)\left(1 - \frac{Q_{P\,min}}{q_P}\right)\left(\frac{G}{K_{sG} + G}\right), \quad (1)$$

$$\rho(N, q_N) = \rho_{N\,max}\ \frac{N}{K_{sN} + N}\left(1 - \frac{q_N}{Q_{N\,max}}\right), \quad (2)$$

$$\rho(P, q_P) = \rho_{P\,max}\ \frac{P}{K_{sP} + P}\left(1 - \frac{q_P}{Q_{P\,max}}\right), \quad (3)$$

where μ_{max} (day^{-1}) is the maximum mixotrophic growth rate; N (mg nitrate L^{-1}), P (mg phosphate L^{-1}), and G (g glucose L^{-1}) are the

nitrate, phosphate, and glucose concentrations in the medium as the sole nitrogen, phosphorus and organic carbon sources, respectively; q_N (gN gC^{-1}) and q_P (gP gC^{-1}) are the internal nitrogen and phosphorus quotas. $\rho_{N\,max}$ (gN gC^{-1} day^{-1}) and $\rho_{P\,max}$ (gP gC^{-1} day^{-1}) represent the maximum nitrogen uptake rates; $Q_{N\,min}$ (gN gC^{-1}) and $Q_{P\,min}$ (gP gC^{-1}) are the minimum quotas of nitrogen and phosphorus, below which growth cannot occur; $Q_{N\,max}$ (gN gC^{-1}) and $Q_{P\,max}$(gP gC^{-1}) are the maximum quotas for nitrogen and phosphorus, above which nutrient uptake stops; and K_{sN} (mg nitrate L^{-1}), K_{sP} (mg phosphate L^{-1}), and K_{sG} (g glucose L^{-1}) represent the half-saturation constants for nitrate, phosphate and glucose, respectively.

Description of lutein production was introduced as a separate state variable based on Luedeking–Piret kinetic model (Luedeking & Piret, 1959), proven effective in previous studies (Wu et al., 2007; Zhang et al., 1999). This model represents the lutein formation rate of cells as a combination of a growth-associated constant α (mg lutein g $cells^{-1}$) and a nongrowth-associated constant β (mg lutein g $cells^{-1}$ day^{-1}). α represents the instantaneous yield of lutein formation due to cell growth, whereas β represents the specific rate of product formation.

The complete model structure integrates seven state variables: biomass (X, g cells L^{-1}), internal nitrogen quota (q_N, gN gC^{-1}), internal phosphorus quota (q_P, gP gC^{-1}), nitrate (N, mg nitrate L^{-1}), phosphate (P, mg phosphate L^{-1}), glucose (G, g glucose L^{-1}) and lutein (L, mg lutein L^{-1}) as follows (Equation (4)):

$$\begin{cases} \frac{dX}{dt} = \mu(q_N, q_P, G)X \\ \frac{dq_N}{dt} = \rho(N, q_N) - \mu(q_N, q_P, G)q_N \\ \frac{dN}{dt} = -\rho(N, q_N)X \\ \frac{dq_P}{dt} = \rho(P, q_P) - \mu(q_N, q_P, G)q_P \\ \frac{dP}{dt} = -\rho(P, q_P)X \\ \frac{dG}{dt} = -K_G \quad \mu(q_N, q_P, G)X \\ \frac{dL}{dt} = \alpha \quad \mu(q_N, q_P, G)X + \beta X \end{cases} . \tag{4}$$

Estimating model parameters in complex, multifactorial models is known to be challenging (Bekirogullari et al., 2020; Benavides et al., 2015; Darvehei et al., 2018; Deschênes & Wouwer, 2016; Zhang et al., 1999). As in the earlier model (Bentahar & Deschênes, 2023), a nonlinear least-squares optimization procedure was chosen to estimate the parameters. The optimization process was performed using a combination of the Nelder–Mead and Levenberg–Marquardt methods (Levenberg, 1944; Marquardt, 1963; Nelder & Mead, 1965). The *fminsearch*, *fmincon*, and *lsqnonlin* routines from MATLAB® 2019a were employed to find the optimal parameter values that minimized the difference between experimental data and the model's predictions. The initial parameter guesses were those obtained from the earlier model as the accuracy of such models depends critically on the choice of objective functions and constraints (Ryu et al., 2018).

3 | RESULTS AND DISCUSSION

3.1 | Effects of various concentrations of nitrate and phosphate on biomass production

This study conducted a run of 16 batch cultures to investigate the impacts of nitrate and phosphate concentrations on *T. obliquus* biomass growth and lutein production under mixotrophic conditions. The experiments were duplicated using low and high nitrate and phosphate concentrations. The progress of cell growth over a 12-day period is displayed in Figure 2a–d. Results showed that the biomass concentration significantly increased ($p = 6.2 \times 10^{-82}$) with the increase in initial nitrate concentration up to 912 mg L^{-1} (equivalent to 5× BBM), with a fourfold increase in biomass concentration, ranging from a minimum of 1.69 g L^{-1} to a maximum of 6.80 g L^{-1}. These results are consistent with the literature (Chen, Hsu, et al., 2019), which reported that maximal biomass production increased dramatically with increasing calcium nitrate concentrations. They found the highest biomass production (12.73 g L^{-1}) with a nitrate concentration of 2362.9 mg L^{-1}. These findings support the positive impact of nitrate concentration on biomass growth and highlight the potential for increased biomass production with higher nitrate concentrations. However, an analysis of variance test showed no significant difference ($p = 0.59$) when nitrate concentration was increased from 912 mg L^{-1} to 1824 mg L^{-1} (5× BBM to 10× BBM equivalent). This observation suggests an additional limiting factor (i.e., glucose) being depleted from the medium. On the other hand, no significant difference ($0.05 < p < 0.71$) in biomass production was found with the increase in phosphate concentration from 163 mg L^{-1} to 1630 mg L^{-1} (1× BBM to 10× BBM equivalent), except when using a nitrate concentration equivalent to 10× BBM ($p = 3.8 \times 10^{-5}$).

The importance of nitrogen (N) concentration in the culture medium for *T. obliquus* growth is well established (Bentahar & Deschênes, 2022). However, phosphorus (P) is also essential for microalgal growth. It is crucial to synthesize cellular components such as the cell membrane, DNA, RNA, and ATP (Atiku et al., 2016). Previous studies have shown that P deficiency in the culture medium reduces *T. obliquus* growth (Akgül & Akgül, 2022; Xin et al., 2010). N–P coupling has also been found to have a significant effect on nutrient uptake, dry mass, and pigments (Huang et al., 2021). Beuckels et al. (2015) reported that *T. obliquus* adjusts its N and P concentrations based on the supply in the medium, with high N concentrations being crucial for effective P uptake. This study complements these findings by highlighting the dynamics of biomass production under a broad spectrum of growth conditions and providing a mathematical kinetic model to describe this process. The results suggest that while N concentration has a significant impact on biomass production, P concentration may not have a direct impact under mixotrophic conditions. However, the combination of N and P concentrations may still significantly impact *T. obliquus* growth and further investigation is required to explore this interaction. The findings suggest that higher nitrate concentrations could be used to

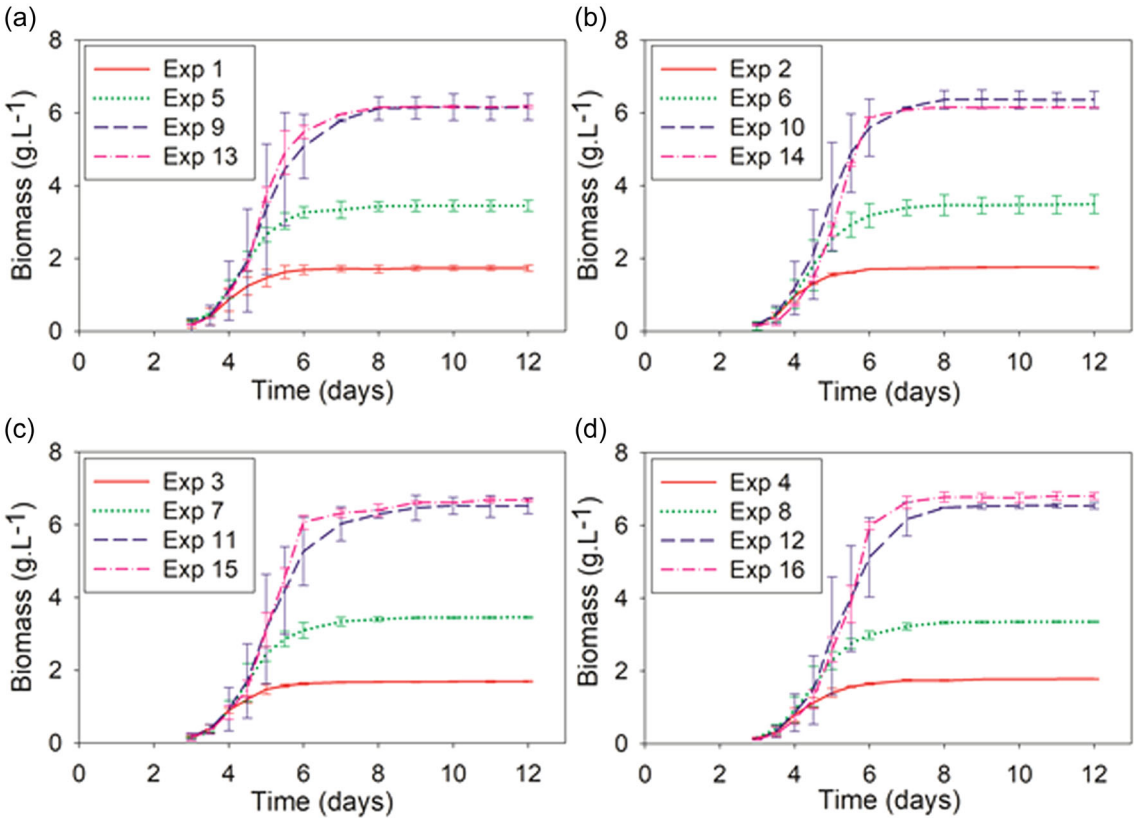

FIGURE 2 Changes in biomass concentration across 16 experimental variations. Solid, dotted, dashed, and dotted-dashed lines represent the four initial nitrate concentrations equivalent to 1×, 2×, 5×, and 10× Bold's Basal Medium (BBM), respectively. (a–d) Corresponds to the four initial phosphate concentrations equivalent to 1×, 2×, 5×, and 10× BBM, respectively. Mean ± SD (n = 2) is shown.

increase *T. obliquus* biomass production, but this must be balanced against the cost of the added nutrients.

3.2 | Effects of various concentrations of nitrate and phosphate on lutein production

The dynamic changes in lutein concentration were studied under varying nitrate and phosphate conditions, as displayed in Figure 3a–d. Results indicated a significant increase in lutein concentration as the initial nitrate concentration was raised from 182.4 to 1824 mg.L^{-1} ($p = 3.6 \times 10^{-97}$), resulting in a 12-fold increase in final lutein concentration from 2.13 mg L^{-1} (Experiment 1) to 25.58 mg L^{-1} (Experiment 16). However, no significant correlation was observed between changes in phosphate concentration and lutein production ($0.055 < p < 0.76$), except when using a nitrate concentration equivalent to 10× BBM ($p = 0.007$). This suggests that phosphate supplementation alone has a limited impact on lutein production, whereas elevated nitrate concentration has a significant effect. Notably, this study demonstrated higher lutein concentrations than previous studies in *T. obliquus* under mixotrophic and autotrophic conditions, with a maximum lutein concentration of 8.2 and 5.6 mg L^{-1}, respectively (Chen, Hsu, et al., 2019; Yen et al., 2011). This might be due to the effect of nitrogen availability, as nitrogen is critical in maximizing lutein accumulation in microalgae (Chen, Hsu, et al., 2019; Henríquez et al., 2016). Increasing the nitrogen concentration can improve lutein synthesis under optimal light supply, even though lutein does not require nitrogen for synthesis (Zheng et al., 2022).

Regarding lutein yields and productivities, results showed a range of lutein yield from 1.17 to 4.08 mg g^{-1} and lutein productivity from 0.18 to 2.13 mg L^{-1} day^{-1}, which compares favorably with previous studies. For instance, lutein content of 1.5 mg g^{-1} and yield of 3.06 mg L^{-1} day^{-1} were achieved in mixotrophic cultivation of *T. obliquus* with 2% glucose and 4.5 g L^{-1} calcium nitrate (Chen, Hsu, et al., 2019). Additionally, under mixotrophic conditions using 6 g L^{-1} crude glycerol and a 20:1 N/P ratio, maximum lutein productivity of 3.59 mg L^{-1} day^{-1} was reported (Rajendran et al., 2020). Other factors, such as mode of nutrition and light source and intensity, have also been investigated for their impact on lutein production in microalgae. Autotrophic cultivation was found to be more favorable for lutein production in *T. obliquus*, yielding a higher lutein productivity of 0.44 mg L^{-1} day^{-1} compared with mixotrophic cultivation with 3 g L^{-1} glycerol supplementation (0.36 mg L^{-1} day^{-1}) after 7 days of cultivation (Yen et al., 2011). Furthermore, Ho et al. (2014) reported that optimizing the light source and intensity improved lutein productivity in *T. obliquus* by three times, from 1.39 to 4.15 mg L^{-1} day^{-1}. White light at an intensity of 300 µmol m^{-2} s^{-1} was found to be the most favorable for lutein production, with the highest content (4.52 mg g^{-1})

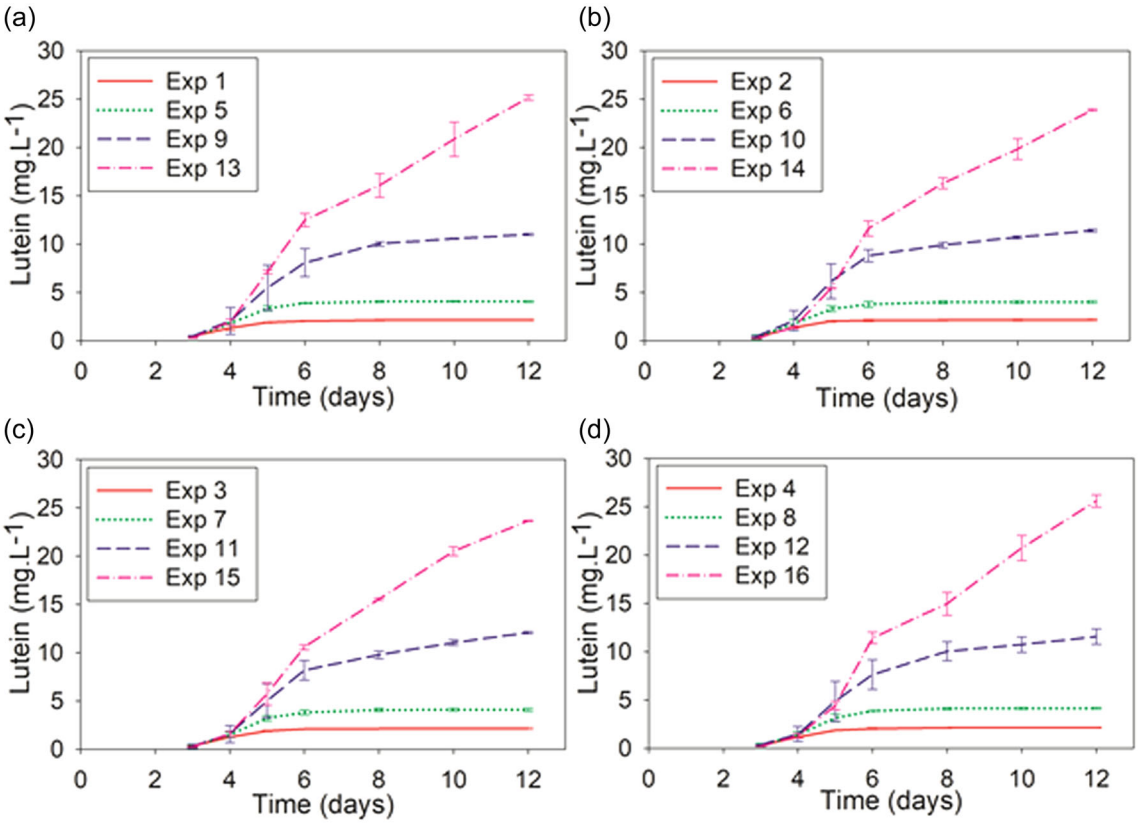

FIGURE 3 Lutein concentration trends for 16 experimental variations. Solid, dotted, dashed, and dotted-dashed lines represent the four initial nitrate concentrations equivalent to 1×, 2×, 5×, and 10× Bold's Basal Medium (BBM), respectively. (a–b) correspond to the four initial phosphate concentrations equivalent to 1×, 2×, 5×, and 10× BBM, respectively. Mean ± SD (n = 2) is shown.

and productivity (4.15 mg L^{-1} day^{-1}). In contrast, red light had the lowest lutein accumulation, with 3–4 mg g^{-1} compared with blue, green, and white lights. Overall, the findings of this study suggest that the optimization of nitrogen availability is crucial for maximizing lutein accumulation in *T. obliquus* and can contribute to the development of efficient strategies for the commercial production of this valuable pigment from microalgae.

3.3 | Results of model construction and parameters estimation

To thoroughly investigate the impact of nitrate concentration on the parameters of this model, the experimental data were categorized into four groups based on initial nitrate levels (1×, 2×, 5×, and 10× BBM). The model consisted of 16 batch experiments (run in duplicate), with each nitrate level category having three duplicate experiments for calibration and one duplicate experiment for validation (Table 3). This resulted in a total of 12 experiments used for calibration and four experiments kept for validation, both run twice. The proposed model (Equation [4]) was calibrated for each group to estimate 13 parameters that describe changes in biomass, internal nitrogen quota, internal phosphorus quota, nitrate, phosphate, glucose, and lutein. The estimated values of each kinetic parameter were determined using a nonlinear least-squares optimization procedure as described in Section 2.4.

The results (Table 4) showed that the estimated parameter values were largely consistent across the four nitrate level categories, except for the nongrowth-associated parameter β, which increased substantially under higher initial nitrate concentrations. Specifically, the value of β rose from 0.0001 at 1× and 2× BBM to 0.06 at 5× BBM, and further increased to 0.35 at 10× BBM. This increase could be due to lutein synthesis being influenced by other factors such as light and environmental conditions, rather than strictly controlled by the cellular growth rate. However, values for β were much smaller than α, indicating that lutein was primarily associated with growth, in contrast to other algal species such as *Chlorella minutissima*, where lutein was nongrowth associated (De Bhowmick et al., 2019). Considering the possibility of expressing the β parameter as a function of environmental conditions, such as nitrate, rather than a constant appeared to be a more promising approach. However, further experimental validation is needed, which could be addressed in future work.

On the other hand, the parameters acquired in the previous study (Bentahar & Deschênes, 2023) did not facilitate an optimal fit for the new data, as they were employed as initial guesses. A reevaluation of the maximum specific growth rate μ_{max} for *T. obliquus* resulted in a revised value of 4.03 day^{-1}, a notable increase compared with the previous model's value of 1.45 day^{-1}. This adjustment

TABLE 4 Estimated parameter values from model calibration for four initial nitrate concentrations.

Model parameter	Units	Initial nitrate concentration (mg L^{-1}) 182.4 (BBM 1×)	364.8 (BBM 2×)	912 (BBM 5×)	1824 (BBM 10×)
μ_{max}	day^{-1}	4.0377	4.0316	4.0712	4.0822
$\rho_{N\,max}$	gN gC^{-1} day^{-1}	0.9798	0.9805	0.9765	0.9811
$\rho_{P\,max}$	gP gC^{-} day^{-1}	0.6000	0.6007	0.6000	0.6000
$Q_{N\,max}$	gN gC^{-1}	0.1652	0.1659	0.1648	0.1669
$Q_{N\,min}$	gN gC^{-1}	0.0560	0.0567	0.0484	0.0432
$Q_{P\,max}$	gP gC^{-1}	0.0820	0.0820	0.0825	0.0820
$Q_{P\,min}$	gP gC^{-1}	0.0028	0.0029	0.0023	0.0035
K_{sN}	mg nitrate L^{-1}	134.9700	134.6600	135.1500	135.0200
K_{sP}	mg phosphate L^{-1}	81.1310	81.1920	81.7280	81.9980
K_{sG}	g glucose L^{-1}	8.2684	8.3573	7.5194	7.3911
K_G	g glucose gC^{-1}	2.9963	2.9973	2.9999	3.0000
α	mg lutein g $cells^{-1}$	1.2525	1.2525	1.2525	1.2525
β	mg lutein g $cells^{-1}$ day^{-1}	0.0001	0.0001	0.0649	0.3538

Abbreviation: BBM, Bold's Basal Medium.

appears to be more suitable for mixotrophic cultivation leading to higher half-saturation constants for all substrates (i.e., nitrate, phosphate, and glucose). The newly determined μ_{max} surpasses the cumulative values reported for photoautotrophic (1.47 day^{-1}) and heterotrophic (1.8 day^{-1}) cultivation conditions (Deschênes & Wouwer, 2016; Di Caprio et al., 2019). These findings support the hypothesis that the specific growth rate in mixotrophic conditions is not simply a sum of those in photoautotrophic and heterotrophic modes, but rather involves synergistic effects of both metabolic processes (Fernández et al., 2013; Salati et al., 2017).

Additionally, the microalgae exhibited a higher demand for nitrogen than phosphorus, as reflected by their higher nitrogen uptake rates and higher minimum and maximum internal nitrogen quotas. This preference indicates that the microalgae may not reach their maximum potential growth rate due to a nitrogen limitation, highlighting the importance of maintaining a balance between both nitrogen and phosphorus to ensure optimal microalgal growth and productivity. Moreover, glucose availability could be another limiting factor for the microalgae's growth rate, as the half-saturation constant for glucose uptake (K_{sG}) was found to be higher than that for nitrate uptake (K_{sN}). Maintaining an appropriate balance between nitrogen and phosphorus availability while ensuring sufficient glucose concentration could contribute to achieving optimal growth conditions and enhancing microalgal productivity.

Figure 4a–g shows the results of fitting the model to data for different initial nitrate levels (Runs #2, 7, 12, and 13), which are representative of the overall data set. Although only a subset of results was presented due to space limitations, all other fits are similar (see Supporting Information S1: Figures S1–S12 available in Section 1). The degree of model fit was evaluated by calculating the correlation coefficient (R^2) for experimental and calibrated data concerning different nutrient utilization profiles, along with biomass and lutein formations. The present model exhibited improved calibration for utilization profiles of nitrate ($R^2 > 0.96$), phosphate ($R^2 > 0.95$), and glucose ($R^2 > 0.94$) as compared with our previous model (Bentahar & Deschênes, 2023), for which the corresponding R^2 values were above 0.78, 0.81, and 0.82, respectively. The high correlation coefficients indicated that the calibration equations could be regarded as sufficient to describe the effect of different substrate consumption. Additionally, the model proved to represent experimental data accurately to describe the mixotrophic growth and lutein production of *T. obliquus* with $R^2 > 0.95$ for all cases. The consistency of the estimated parameter values suggests the combination of the Nelder–Mead and Levenberg–Marquardt methods to be effective for solving nonlinear problems with noisy cost functions. In addition, the relatively high volume of experimental data, consisting of 86-point duplicated results for each condition, enhances the reliability of the parameter values, given the number of model parameters (13). Overall, these findings suggested the model to be applied under a broad range of conditions, providing valuable reference data and supplementing existing literature. The following section discusses the validation of the model.

3.4 | Validation of kinetic model predictability

To validate the model, a separate set of experimental data was used, distinct from the data utilized to estimate the unknown parameters for each initial nitrate concentration, as described in Section 3.3. Specifically, the data obtained from duplicate batch experiments in

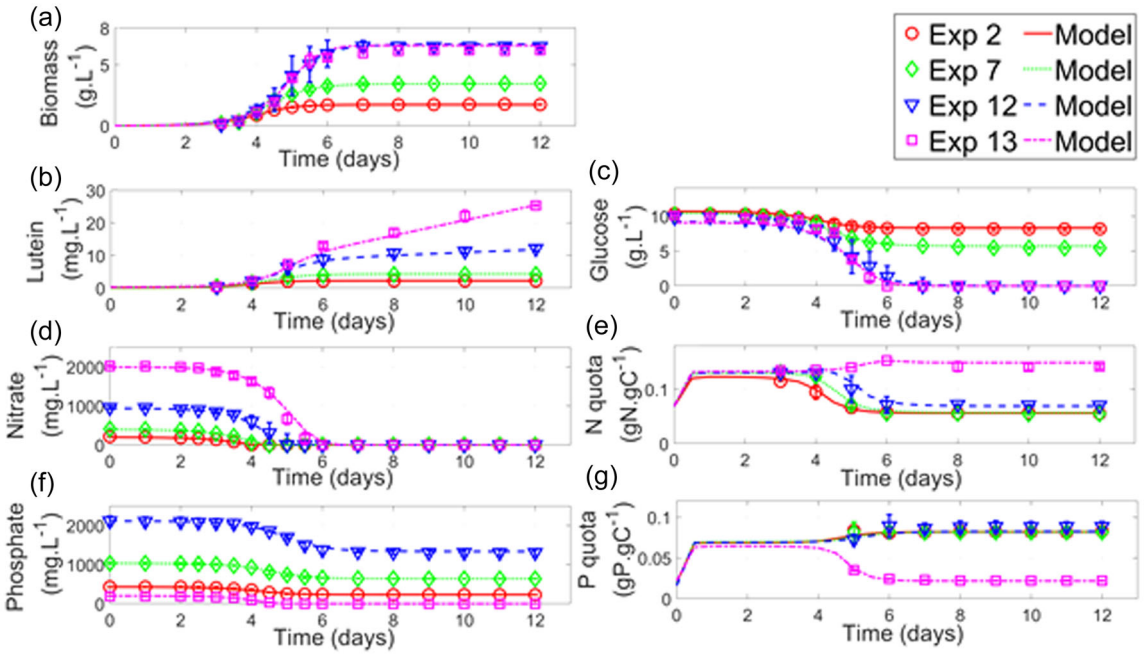

FIGURE 4 Calibration results of proposed model compared with experimental data for the production of biomass (a) and lutein (b), the consumption of glucose (c), nitrate (d), and phosphate (f), and the internal nitrogen (e) and phosphorus (g) quotas. Model simulations for four initial nitrate levels (1×, 2×, 5×, 10× Bold's Basal Medium [BBM]) are shown as solid, dotted, dashed, and dotted-dashed lines, and correspond to the experimental results symbolized by circles, diamonds, triangles, and squares. Results are presented as mean ± SD ($n = 2$). Only four representative experiments per nitrate level are shown (2, 7, 12, and 13), whereas all duplicates can be found in Supporting Information S1: Section 1.

Runs #4, 6, 9, and 15 (1×, 2×, 5×, and 10× BBM equivalent, respectively) were reserved for model validation, rather than calibration. Figure 5a–g illustrates the model's predictive capabilities for each state variable, with one representative example per experimental condition shown, and all duplicates simulated individually (see Supporting Information S1: Figures S13–S16 available in Section 2 of for details). The previously identified model parameters were used in these tests, whereas initial conditions for the model states were estimated from the new experimental data. As expected, the model was able to accurately predict the dynamic concentration profiles for biomass ($0.88 < R^2 < 0.98$) and lutein ($0.78 < R^2 < 0.95$) formations across various nitrate and phosphate concentration regimes.

The data analysis from model calibration and validation profiles (Figures 4a,b and 5a,b) demonstrates that nitrogen concentration has a significant impact on both cell growth and lutein formation, which is consistent with previous studies (Akgül & Akgül, 2022; Bentahar & Deschênes, 2022). Nitrogen plays a crucial role in algal growth, as it is a fundamental component of various biomolecules that are essential for cellular processes, including enzymes, chlorophylls, genetic material, and energy transfer molecules (Kim et al., 2016). This study also found that increasing the initial nitrate concentration leads to higher cell density, which, in turn, causes self-shading and limits light availability during the later stages of growth. This effect, in turn, enhances lutein production, as lutein is required for maintaining the structural integrity of light-harvesting complexes (LHCs) that promote photosynthesis under low light conditions (Zheng et al., 2022). The increase in lutein content due to nitrogen enrichment is consistent with previous studies on other microalgal strains (Chen, Hsu, et al., 2019; Cordero et al., 2011; Ho et al., 2015; Xie et al., 2013). The multiplicative model used in this study did not consider the influence of light and self-shading. Previous models have addressed the impact of self-shading on microalgae growth resulting from light attenuation in dense cultures (Bernard et al., 2009; Deschênes & Wouwer, 2016; Quinn et al., 2011; Yuan et al., 2014). Additionally, Ho et al. (2014) demonstrated a threefold improvement in lutein productivity in *T. obliquus* through the optimization of light source and intensity. Future research should incorporate these factors into the existing model for a better understanding of their effects on biomass and pigment production.

In addition, the model accurately predicted substrate consumption yields for glucose ($0.87 < R^2 < 0.99$), nitrate ($0.83 < R^2 < 0.99$), and phosphate ($0.85 < R^2 < 0.99$) concentrations, indicating that the multiplicative method utilizing Monod and Droop-based expressions is a suitable approach for describing substrate uptake dynamics. The consumption of glucose follows a similar trend as the growth of microalgae, supporting the use of the Monod equation to describe the effect of glucose on the mixotrophic growth of *T. obliquus* (Figures 4c and 5c). The lower glucose consumption yields observed in cultures grown under low nitrate concentrations might be related to an imbalance in the C/N ratio, which is known to be close to the Redfield ratio (around 6.6) (Islam et al., 2019). The high C/N ratio in the low-nitrate cultures (about 16.2 and 8.1 for initial nitrate concentrations of 1× and 2× BBM, respectively) suggests a potential

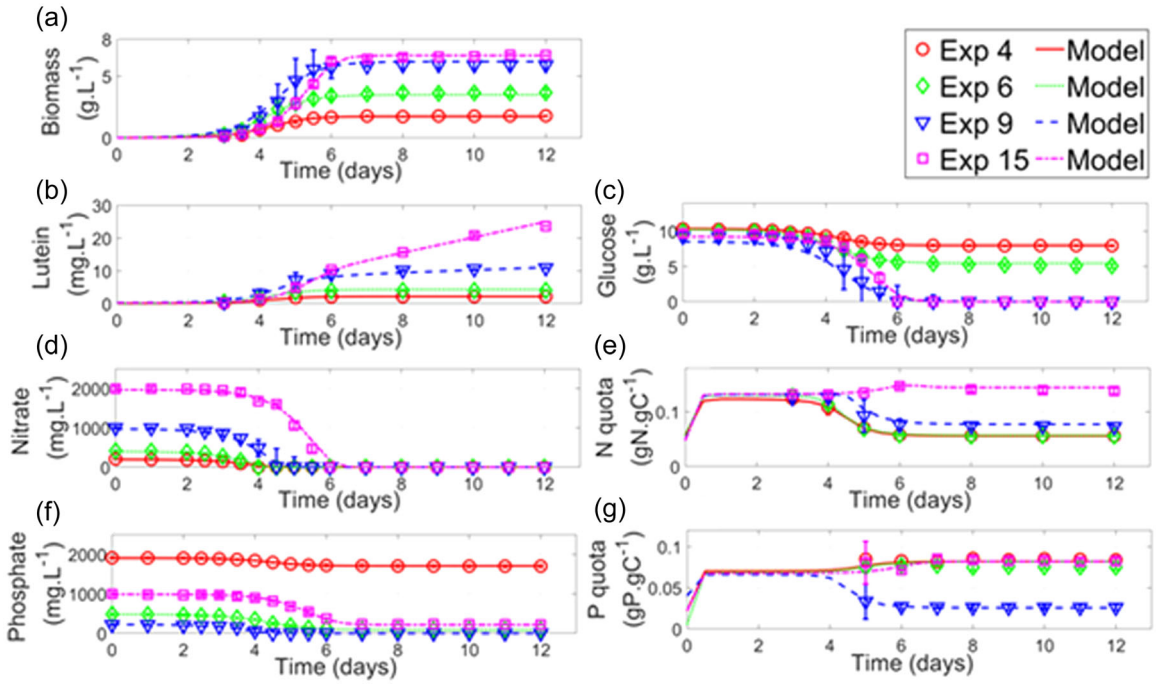

FIGURE 5 Comparison of model prediction with validation experiments (4, 6, 9, and 15) for the production of biomass (a) and lutein (b), the consumption of glucose (c), nitrate (d), and phosphate (f), and the internal nitrogen (e) and phosphorus (g) quotas. Model simulations for four initial nitrate levels (1×, 2×, 5×, 10× Bold's Basal Medium [BBM]) are shown as solid, dotted, dashed, and dotted-dashed lines, and correspond to the experimental results symbolized by circles, diamonds, triangles, and squares, respectively. Results are presented as mean ± SD ($n = 2$). Only one of the duplicates per experimental condition is represented here, but the simulation of all duplicates is available in Supporting Information S1: Section 2.

N limitation, which could explain why glucose was not fully consumed. Conversely, the low C/N ratio in the high-nitrate cultures (about 3.2 and 1.6 for initial nitrate concentrations of 5× and 10× BBM, respectively) suggests a potential C limitation. On the other hand, the simulated nitrate consumption profile agrees with experimental data (Figures 4d and 5d). Under low initial nitrate concentrations (1× and 2× BBM equivalent), microalgae growth persisted after nitrate exhaustion, suggesting significant intracellular nitrogen accumulation. A similar phenomenon was observed after phosphate exhaustion at a concentration equivalent to 1× BBM (Figures 4f and 5f). The superiority of the Droop equation in describing phosphate consumption is evident, with higher R^2 values in the range of 0.85–0.99. This stands in contrast to the Monod equation ($0.77 < R^2 < 0.92$) employed in the earlier model (Bentahar & Deschênes, 2023). These results align with previous studies indicating that *T. obliquus* cells can utilize intracellular nitrogen and phosphorus after external nutrient exhaustion (Deschênes & Wouwer, 2016; Wu et al., 2013). Thus, the Droop model, which allows to capture the observed ability of microalgae to grow even after complete exhaustion of a limiting nutrient (Figueroa-Torres et al., 2017), yields good trajectories to describe the effect of nitrate and phosphate on the mixotrophic growth of this microalga.

However, minor disagreements between predictions and experimental data can be seen for internal nitrogen and phosphorus quotas dynamics (Figure 5e,g). This observation could result from limited experimental data, as only 7 and 8-point data for each experimental run were used, whereas 13 model parameters were considered. In addition, the measurement of internal quotas is challenging, with potential sources of error such as the numerous experimental steps required for nitrogen quota measurements and the reliance on biomass estimation for phosphorus quota measurements (Bentahar & Deschênes, 2023; Deschênes & Wouwer, 2016; Wu et al., 2013). According to Bougaran et al. (2010), the internal quota of a nutrient is at a minimum level when it limits cellular growth. However, when the same nutrient becomes abundant and another nutrient becomes limiting, the cell accumulates the previously nonlimiting nutrient up to a maximal quota. The observed disagreements between predictions and experimental data might reflect the complex nature of the internal nutrient storage system.

In general, the validation results indicated that the model could describe the relationship between estimated parameters and state variables within the range of variables reported in Table 2, confirming its potential for practical implementation in future applications.

4 | CONCLUSIONS

The multinutrient kinetic model presented in this study offers valuable insights into the interplay of nitrate, phosphate, and glucose in regulating the growth and lutein production of *T. obliquus* species. The model was designed to integrate seven state variables and 13 unknown parameters, estimated using a distinctive experimental design involving a 10-fold variation in nitrate and phosphate

concentrations. The parameter estimation was carried out using nonlinear least-squares optimization techniques, objective functions, and constraints, leading to consistent and robust parameter values.

The investigation revealed significant findings regarding the impact of nitrate and phosphate on microalgal growth and lutein production. Notably, increasing the initial nitrate concentration resulted in a remarkable boost in both biomass and lutein production, achieving up to fourfold and 12-fold increases, respectively. In contrast, phosphate supplementation exhibited a limited influence on microalgal growth and lutein production. Furthermore, the study emphasized the critical role of maintaining a balanced nitrogen–phosphorus ratio, whereas ensuring adequate glucose concentration to optimize microalgal productivities.

The model predicted a wide range of biomass (up to 6.80 g L^{-1}) and lutein (up to 25.58 mg L^{-1}) yields, demonstrating its accuracy and wide applicability within the scope of this investigation. This research holds significant potential for advancing microalgal cultivation techniques and serving as a valuable guideline for similar microalgal cultivation systems, whereas also contributing to an eventual commercial-scale production of lutein and other valuable microalgal products. Future work will focus on developing real-time operation strategies for photobioreactors, including precise real-time automatic control and optimization for large-scale cultivation processes.

ACKNOWLEDGMENTS

This work was supported by the Natural Sciences and Engineering Research Council of Canada under grant number RGPIN-2017-06202 and the Institute for Nutrition and Functional Foods under grant number FRQNT-203315, which the authors gratefully acknowledge.

CONFLICT OF INTEREST STATEMENT

The authors declare no conflict of interest.

DATA AVAILABILITY STATEMENT

The data that support the findings of this study are available from the corresponding author upon reasonable request.

ORCID

Jihed Bentahar http://orcid.org/0000-0002-2897-0207

REFERENCES

Akgül, F., & Akgül, R. (2022). Combined effect of nitrogen and phosphorus on growth and biochemical composition of *Tetradesmus obliquus* (Turpin) M.J. Wynne. *International Journal of Secondary Metabolite*, *9*(4), 525–537. https://doi.org/10.21448/ijsm.1102592

Atiku, H., Mohamed, R., Al-Gheethi, A., Wurochekke, A., & Kassim, A. H. M. (2016). Harvesting of microalgae biomass from the phycoremediation process of greywater. *Environmental Science and Pollution Research*, *23*(24), 24624–24641. https://doi.org/10.1007/s11356-016-7456-9

Bekirogullari, M., Figueroa-Torres, G. M., Pittman, J. K., & Theodoropoulos, C. (2020). Models of microalgal cultivation for added-value products - A review. *Biotechnology Advances*, *44*):107609. https://doi.org/10.1016/j.biotechadv.2020.107609

Benavides, M., Telen, D., Lauwers, J., Logist, F., Van Impe, J., & Wouwer, A. V. (2015). Parameter identification of the droop model using optimal experiment design. *IFAC-PapersOnLine*, *48*(1), 586–591. https://doi.org/10.1016/j.ifacol.2015.05.094

Bentahar, J., & Deschênes, J. S. (2022). Media optimization design towards maximizing biomass production of *Tetradesmus obliquus* under mixotrophic conditions. *Bioresource Technology Reports*, *17*):100885. https://doi.org/10.1016/j.biteb.2021.100885

Bentahar, J., & Deschênes, J. S. (2023). A reliable multi-nutrient model for the rapid production of high-density microalgal biomass over a broad spectrum of mixotrophic conditions. *Bioresource Technology*, *381*):129162. https://doi.org/10.1016/j.biortech.2023.129162

Bernard, O., Masci, P., & Sciandra, A. (2009). A photobioreactor model in nitrogen limited conditions. In: *Mathmod 09-6th Vienna International Conference on Mathematical Modelling*, 1521–1530. https://hal.science/hal-03523391

Beuckels, A., Smolders, E., & Muylaert, K. (2015). Nitrogen availability influences phosphorus removal in microalgae-based wastewater treatment. *Water Research*, *77*, 98–106. https://doi.org/10.1016/j.watres.2015.03.018

Bougaran, G., Bernard, O., & Sciandra, A. (2010). Modeling continuous cultures of microalgae colimited by nitrogen and phosphorus. *Journal of Theoretical Biology*, *265*(3), 443–454. https://doi.org/10.1016/j.jtbi.2010.04.018

Chen, J. H., Chen, C. Y., Hasunuma, T., Kondo, A., Chang, C. H., Ng, I. S., & Chang, J. S. (2019). Enhancing lutein production with mixotrophic cultivation of *Chlorella sorokiniana* MB-1-M12 using different bioprocess operation strategies. *Bioresource Technology*, *278*, 17–25. https://doi.org/10.1016/j.biortech.2019.01.041

Chen, W. C., Hsu, Y. C., Chang, J. S., Ho, S. H., Wang, L. F., & Wei, Y. H. (2019). Enhancing production of lutein by a mixotrophic cultivation system using microalga *Scenedesmus obliquus* CWL-1. *Bioresource Technology*, *291*, 121891. https://doi.org/10.1016/j.biortech.2019.121891

Cordero, B. F., Obraztsova, I., Couso, I., Leon, R., Vargas, M. A., & Rodriguez, H. (2011). Enhancement of lutein production in *Chlorella sorokiniana* (chorophyta) by improvement of culture conditions and random mutagenesis. *Marine Drugs*, *9*(9), 1607–1624. https://doi.org/10.3390/md9091607

Darvehei, P., Bahri, P. A., & Moheimani, N. R. (2018). Model development for the growth of microalgae: A review. *Renewable and Sustainable Energy Reviews*, *97*, 233–258. https://doi.org/10.1016/j.rser.2018.08.027

De Bhowmick, G., Sen, R., & Sarmah, A. K. (2019). Analysis of growth and intracellular product synthesis dynamics of a microalga cultivated in wastewater cocktail as medium. *Biochemical Engineering Journal*, *149*):107253. https://doi.org/10.1016/j.bej.2019.107253

Deschênes, J. S., & Wouwer, A. V. (2016). Parameter identification of a dynamic model of cultures of microalgae *Scenedesmus obliquus* - an experimental study. *IFAC-PapersOnLine*, *49*(7), 1050–1055. https://doi.org/10.1016/j.ifacol.2016.07.341

Di Caprio, F., Altimari, P., Ianquaniello, G., Toro, L., & Pagnanelli, F. (2019). *T. obliquus* cultivation under heterotrophic conditions: Determination of growth parameters. *Chemical Engineering Transactions*, *74*, 133–138. https://doi.org/10.3303/CET1974023

Droop, M. R. (1968). Vitamin B12 and marine ecology. IV. The kinetics of uptake, growth and inhibition in *Monochrysis lutheri*. *Journal of the Marine Biological Association of the United Kingdom*, *48*(3), 689–733. https://doi.org/10.1017/S0025315400019238

Fernández, F. G. A., Sevilla, J. M. F., & Grima, E. M. (2013). Photobioreactors for the production of microalgae. *Reviews in Environmental Science and Bio/Technology*, *12*(2), 131–151. https://doi.org/10.1007/s11157-012-9307-6

Figueroa-Torres, G. M., Pittman, J. K., & Theodoropoulos, C. (2017). Kinetic modelling of starch and lipid formation during mixotrophic, nutrient-limited microalgal growth. *Bioresource Technology*, *241*, 868–878. https://doi.org/10.1016/j.biortech.2017.05.177

Guedes, A. C., Amaro, H. M., & Malcata, F. X. (2011). Microalgae as sources of high added-value compounds-A brief review of recent work. *Biotechnology Progress*, *27*(3), 597–613. https://doi.org/10.1002/btpr.575

Henríquez, V., Escobar, C., Galarza, J., & Gimpel, J. (2016). Carotenoids in microalgae, *Carotenoids in nature, subcellular biochemistry* (Vol. 79, pp. 219–237). Springer International Publishing. https://doi.org/10.1007/978-3-319-39126-7_8

Ho, S. H., Chan, M. C., Liu, C. C., Chen, C. Y., Lee, W. L., Lee, D. J., & Chang, J. S. (2014). Enhancing lutein productivity of an indigenous microalga *Scenedesmus obliquus* FSP-3 using light-related strategies. *Bioresource Technology*, *152*, 275–282. https://doi.org/10.1016/j.biortech.2013.11.031

Ho, S. H., Xie, Y., Chan, M. C., Liu, C. C., Chen, C. Y., Lee, D. J., Huang, C. C., & Chang, J. S. (2015). Effects of nitrogen source availability and bioreactor operating strategies on lutein production with *Scenedesmus obliquus* FSP-3. *Bioresource Technology*, *184*, 131–138. https://doi.org/10.1016/j.biortech.2014.10.062

Huang, Y., Lou, C., Luo, L., & Wang, X. C. (2021). Insight into nitrogen and phosphorus coupling effects on mixotrophic *Chlorella vulgaris* growth under stably controlled nutrient conditions. *Science of the Total Environment*, *752*, 141747. https://doi.org/10.1016/j.scitotenv.2020.141747

Islam, M. J., Jang, C., Eum, J., Jung, S., Shin, M. S., Lee, Y., Choi, Y., & Kim, B. (2019). C:N:P stoichiometry of particulate and dissolved organic matter in river waters and changes during decomposition. *Journal of Ecology and Environment*, *43*(1), 4. https://doi.org/10.1186/s41610-018-0101-4

Kim, G., Mujtaba, G., & Lee, K. (2016). Effects of nitrogen sources on cell growth and biochemical composition of marine chlorophyte *Tetraselmis* sp. For lipid production. *Algae*, *31*(3), 257–266. https://doi.org/10.4490/algae.2016.31.8.18

Levenberg, K. (1944). A method for the solution of certain non-linear problems in least squares. *Quarterly of Applied Mathematics*, *2*(2), 164–168.

Luedeking, R., & Piret, E. L. (1959). A kinetic study of the lactic acid fermentation. Batch process at controlled pH. *Journal of Biochemical and Microbiological Technology and Engineering*, *1*(4), 393–412.

Marquardt, D. W. (1963). An algorithm for least-squares estimation of non-linear parameters. *Journal of the Society for Industrial and Applied Mathematics*, *11*(2), 431–441. https://doi.org/10.1137/0111030

Monod, J. (1949). The growth of bacterial cultures. *Annual Review of Microbiology*, *3*(1), 371–394.

Nelder, J. A., & Mead, R. (1965). A simplex method for function minimization. *The Computer Journal*, *7*(4), 308–313. https://doi.org/10.1093/comjnl/8.1.27

Oliveira, C. Y. B., Oliveira, C. D. L., Prasad, R., Ong, H. C., Araujo, E. S., Shabnam, N., & Gálvez, A. O. (2021). A multidisciplinary review of *Tetradesmus obliquus*: a microalga suitable for large-scale biomass production and emerging environmental applications. *Reviews in Aquaculture*, *13*(3), 1594–1618. https://doi.org/10.1111/raq.12536

Quinn, J., de Winter, L., & Bradley, T. (2011). Microalgae bulk growth model with application to industrial scale systems. *Bioresource Technology*, *102*, 5083–5092. https://doi.org/10.1016/j.biortech.2011.01.019

Rajendran, L., Nagarajan, N. G., & Karuppan, M. (2020). Enhanced biomass and lutein production by mixotrophic cultivation of *Scenedesmus* sp. using crude glycerol in an airlift photobioreactor. *Biochemical Engineering Journal*, *161*, 107684. https://doi.org/10.1016/j.bej.2020.107684

del Rio-Chanona, E. A., Ahmed, N., Zhang, D., Lu, Y., & Jing, K. (2017). Kinetic modeling and process analysis for *Desmodesmus* sp. lutein photo-production. *AIChE Journal*, *63*(7), 2546–2554. https://doi.org/10.1002/aic.15667

Ryu, K. H., Sung, M. G., Kim, B., Heo, S., Chang, Y. K., & Lee, J. H. (2018). A mathematical model of intracellular behavior of microalgae for predicting growth and intracellular components syntheses under nutrient-replete and -deplete conditions. *Biotechnology and Bioengineering*, *115*(10), 2441–2455. https://doi.org/10.1002/bit.26744

Saha, S. K., Ermis, H., & Murray, P. (2020). Marine microalgae for potential lutein production. *Applied Sciences*, *10*(18), 6457. https://doi.org/10.3390/app10186457

Salati, S., D'Imporzano, G., Menin, B., Veronesi, D., Scaglia, B., Abbruscato, P., Mariani, P., & Adani, F. (2017). Mixotrophic cultivation of *Chlorella* for local protein production using agro-food by-products. *Bioresource Technology*, *230*, 82–89. https://doi.org/10.1016/j.biortech.2017.01.030

Stein, J. R. (1973). *Handbook of phycological methods: Culture methods and growth measurements*. Cambridge University Press.

Wu, Y. H., Li, X., Yu, Y., Hu, H. Y., Zhang, T. Y., & Li, F. M. (2013). An integrated microalgal growth model and its application to optimize the biomass production of *Scenedesmus* sp. LX1 in open pond under the nutrient level of domestic secondary effluent. *Bioresource Technology*, *144*, 445–451. https://doi.org/10.1016/j.biortech.2013.06.065

Wu, Z. Y., Shi, C. L., & Shi, X. M. (2007). Modeling of lutein production by heterotrophic *Chlorella* in batch and fed-batch cultures. *World Journal of Microbiology and Biotechnology*, *23*(9), 1233–1238. https://doi.org/10.1007/s11274-007-9354-2

Xie, Y., Ho, S. H., Chen, C. N. N., Chen, C. Y., Ng, I. S., Jing, K. J., Chang, J. S., & Lu, Y. (2013). Phototrophic cultivation of a thermotolerant *Desmodesmus* sp. for lutein production: Effects of nitrate concentration, light intensity and fed-batch operation. *Bioresource Technology*, *144*, 435–444. https://doi.org/10.1016/j.biortech.2013.06.064

Xin, L., Hong-ying, H., Ke, G., & Ying-xue, S. (2010). Effects of different nitrogen and phosphorus concentrations on the growth, nutrient uptake, and lipid accumulation of a freshwater microalga *Scenedesmus* sp. *Bioresource Technology*, *101*(14), 5494–5500. https://doi.org/10.1016/j.biortech.2010.02.016

Yang, S., Liu, G., Meng, Y., Wang, P., Zhou, S., & Shang, H. (2014). Utilization of xylose as a carbon source for mixotrophic growth of *Scenedesmus obliquus*. *Bioresource Technology*, *172*, 180–185. https://doi.org/10.1016/j.biortech.2014.08.122

Yen, H. W., Sun, C. H., & Ma, T. W. (2011). The comparison of lutein production by *Scenesdesmus* sp. in the autotrophic and the mixotrophic cultivation. *Applied Biochemistry and Biotechnology*, *164*(3), 353–361. https://doi.org/10.1007/s12010-010-9139-1

Yuan, S., Zhou, X., Chen, R., & Song, B. (2014). Study on modelling microalgae growth in nitrogen-limited culture system for estimating biomass productivity. *Renewable and Sustainable Energy Reviews*, *34*, 525–535. https://doi.org/10.1016/j.rser.2014.03.032

Zapata, M., Rodríguez, F., & Garrido, J. (2000). Separation of chlorophylls and carotenoids from marine phytoplankton: A new HPLC method using a reversed phase C8 column and pyridine-containing mobile phases. *Marine Ecology Progress Series*, *195*, 29–45. https://doi.org/10.3354/meps195029

Zhang, X.-W., Shi, X.-M., & Chen, F. (1999). A kinetic model for lutein production by the green microalga *Chlorella protothecoides* in heterotrophic culture. *Journal of Industrial Microbiology & Biotechnology*, *23*, 503–507.

Zheng, H., Wang, Y., Li, S., Nagarajan, D., Varjani, S., Lee, D. J., & Chang, J. S. (2022). Recent advances in lutein production from

microalgae. *Renewable and Sustainable Energy Reviews*, *153*, 111795. https://doi.org/10.1016/j.rser.2021.111795

SUPPORTING INFORMATION

Additional supporting information can be found online in the Supporting Information section at the end of this article.

How to cite this article: Bentahar, J., & Deschênes, J.-S. (2024). A robust multinutrient kinetic model for enhanced lutein and biomass yields in mixotrophic microalgae cultivation: A step towards successful large-scale productions. *Biotechnology and Bioengineering*, *121*, 1596–1608. https://doi.org/10.1002/bit.28663